Calculated and Experimental NMR Chemical Shifts of *p*-Menthane-3,9-diols. A Combination of Molecular Dynamics and Quantum Mechanics to Determine the Structure and the Solvent Effects

Jordi Casanovas,*[,†] Adriana M. Namba,[‡] Salvador León,[§] Gilberto L. B. Aquino,[‡] Gil Valdo José da Silva,*[,‡] and Carlos Alemán*[,||]

Departament de Química, Escola Universitària Politècnica, Universitat de Lleida, c/ Jaume II No. 69, Lleida 25001, Spain, Departamento de Química, Faculdade de Filosofia, Ciência e Letras de Ribeirão Preto, Universidade de São Paulo, Av. Bandeirantes No. 3900, 14040-901, Ribeirão Preto, SP, Brazil, Dipartamento di Chimica "G. Ciamician", Università di Bologna, via Selmi 2, Bologna I-40126, Italy, and Departament d'Enginyeria Química, E.T.S. d'Enginyers Industrials de Barcelona, Universitat Politècnica de Catalunya, Diagonal 647, Barcelona E-08028, Spain

aleman@eq.upc.es

Received December 4, 2000

NMR chemical shifts have been experimentally measured and theoretically estimated for all the carbon atoms of (1*R*,3*S*,4*S*,8*S*)-*p*-menthane-3,9-diol in chloroform solution. Theoretical estimations were performed using a combination of molecular dynamics simulations and quantum mechanical calculations. Molecular dynamics simulations were used to obtain the most populated conformations of the (1*R*,3S:4*S*,8*S*)-*p*-menthane-3,9-diol as well as the distribution of the solvent molecules around it. Quantum mechanical calculations of NMR chemical shifts were performed on the most relevant conformations employing the GIAO-DFT formalism. A special emphasis was put in evaluating the effects of the surrounding solvent molecules. For this purpose, supermolecule calculations were performed on complexes constituted by the solute and *n* chloroform molecules, where *n* ranges from 3 to 16. An excellent agreement with experimental data has been obtained following this computational strategy.

Introduction

The problem of predicting accurate NMR chemical shifts and interpreting them using ab initio quantum mechanical calculations has attracted considerable attention in recent years.[1] Nowadays, theoretical methods such as IGLO,[2] LORG,[3] and GIAO[4] can provide accurate chemical shifts of small molecules in the gas phase.[5] However, it is well-known that these NMR parameters are considerably affected by the chemical environment, i.e., the molecular conformation and the interactions with solvent molecules.[1d]

NMR chemical shift calculations on very flexible compounds such as peptides revealed a strong dependence with the conformation.[6] Molecular geometries required for NMR calculations of small molecules are usually obtained from ab initio calculations or from crystal structures. However, the structure in the crystal can differ considerably from that in solution for flexible molecules, while an ab initio conformational search is difficult or even impracticable for large molecules. On the other hand, solvent effects can be included by continuum models and by supermolecule calculations.[1d] Continuum models take into account only the description of long-range purely electrostatic interactions,[7] whereas the supermolecule approach describes mainly short-range interactions.[8] A recent study about the spectrum of acetylene indicated that coupling constants are mainly affected by long-range interactions, whereas the solvent-induced changes of the NMR chemical shifts are due to short-range specific interactions.[9]

Some difficulties emerge when the supermolecule approach is applied. The most important one is the computational cost of calculations. Therefore, the number of solvent molecules explicitly included in the calculations

* To whom correspondence should be addressed. Additional E-mail adresses: (J.C.) E-mail: JCasanovas@quimica.udl.es. (G.V.J.S.) E-mail: gvjdsilv@usp.br.

† Universitat de Lleida.

‡ Universidade de São Paulo.

§ Università di Bologna.

|| Universitat Politècnica de Catalunya.

(1) (a) Chesnut, D. B. In *Reviews in Computational Chemistry*; Lipkowitz, K. B., Boyd, D. B., Eds.; VCH Publ., Inc.; New York, 1996; Vol. 8; p 245. (b) Jameson, C. J. *Annu. Rev. Phys. Chem.* **1996**, *47*, 135. (c) Schreckenbach, G.; Ziegler, T. *Theor. Chem. Acc.* **1998**, *99*, 71. (d) Helgaker, T.; Jaszunski, M.; Ruud, K. *Chem. Rev.* **1999**, *99*, 293.

(2) (a) Kutzelnigg, W. *Isr. J. Chem.* **1980**, *19*, 193. (b) Kutzelnigg, W.; Fleischer, U.; Schindler, M. *NMR Basic Principles and Progress*; Springer-Verlag: Berlin, 1990; Vol. 23, p 165.

(3) (a) Hansen, A. E.; Bouman, T. D. *J. Chem. Phys.* **1985**, *82*, 5035. (b) Hansen, A. E.; Bouman, T. D. *J. Chem. Phys.* **1989**, *91*, 3552.

(4) (a) Ditchfield, R. *J. Chem. Phys.* **1972**, *56*, 5688. (b) Ditchfield, R. *Mol. Phys.* **1974**, *27*, 789. (c) Pulay, P.; Wolinski, K.; Hinton, J. F. *J. Am. Chem. Soc.* **1990**, *112*, 8251.

(5) (a) Hnyk, D.; Vajda, E.; Bühl, M.; Scheleyer, P. v. R. *Inorg. Chem.* **1992**, *31*, 2464. (b) Mebel, A. M.; Charkin, O. P.; Schleyer, P. v. R. *Inorg. Chem.* **1993**, *32*, 469. (c) Bühl. M.; Thiel, W.; Fleischer, U.; Kuzelnigg, W. *J. Phys. Chem.* **1995**, *99*, 4000. (d) Sundholm, D. *J. Am. Chem. Soc.* **1995**, *117*, 11523. (e) Gauss, J.; Stanton, J. F. *THEOCHEM* **1997**, *398/399*, 73. (f) Jiao, H.; Scheleyer, P. v. R.; Beno, B. R.; Houk, K. N.; Warmuth, R. *Angew. Chem., Int. Ed. Engl.* **1997**, *36*, 2761.

(6) (a) Sulzbach, H. M.; Scheleyer, P. v. R.; Schaefer, H. F., III. *J. Am. Chem. Soc.* **1994**, *116*, 3967−3972. (b) Laws, D. D.; Le, H.; de Dios, A. C.; Havlin, R. H.; Oldfield, E. *J. Am. Chem. Soc.* **1995**, *117*, 9542.

(7) Tomasi, J.; Persico, M. *Chem. Rev.* **1994**, *94*, 2027.

(8) (a) Alemán, C. *Chem. Phys. Lett.* **1999**, *302*, 461. (b) Alemán, C. *Chem. Phys.* **1999**, *244*, 151.

(9) Pecul, M.; Sadlej, J. *Chem. Phys.* **1998**, *234*, 111.

10.1021/jo0016982 CCC: $20.00
Published on Web 05/01/2001

Scheme 1. (1*R*,3*S*,4*S*,8*S*)-*p*-Menthane-3,9-diol

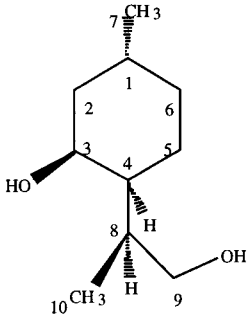

has been usually reduced to one,[9,10] and additionally, supermolecule calculations of realistic systems have been restricted to the Hartree−Fock level.[1d] However, the proper theoretical description of chemical shifts requires electron correlation effects to be included.[1] Furthermore, the number of solvent configurations is very large, and the most representative ones should be included in the clusters built for supermolecule calculations.

In this work, we have investigated the effects of both the geometry and the solvent on the NMR chemical shifts of a complex organic molecule in order to determine its structure. This is the (1*R*,3*S*,4*S*,8*S*)-*p*-menthane-3,9-diol (Scheme 1), which belongs to a family of compounds with considerable interest in many fields of organic chemistry. Thus, *p*-menthane-3,9-diols are obtained from two terpenoids frequently used in the synthesis of natural products, called (−)-isopulegol and (+)-*neo*-isopulegol.[11] As can be seen, (1*R*,3*S*,4*S*,8*S*)-*p*-menthane-3,9-diol consists of a cyclohexane ring with methyl, hydroxyl, and 1-methyl-2-hydroxyethyl substituents attached at C1, C3, and C4 carbon atoms, respectively. The substituents bonded at C3 and C4 are cis to one another, both of them being trans with respect to the methyl group attached to C1. It should be mentioned that the two hydroxyl groups are close in the space conferring an amphiphilic character to the compound. Moreover, in some *p*-methane-3,9-diols these hydroxyl groups form an intramolecular hydrogen bond stabilizing an unusual conformation for the cyclohexane ring.[12]

The goal of the present study is not only to obtain structural information from NMR spectra but also to propose a computational approach to study flexible organic compounds from chemical shift calculations. In this approach, both the conformational preferences of the solute and the most representative configurations of solvent molecules are obtained from molecular dynamics (MD) simulations using empirical potential functions. Shielding properties of the atoms in a magnetic field are then computed by means of ab initio quantum mechanical techniques that include electron correlation effects. This methodology allows us to evaluate accurate NMR chemical shifts not only on the geometry of the lowest energy minimum but also on the geometries of other populated conformers.

Experimental Section

Experimental Methods. ^{1}H NMR spectra were obtained on a Bruker DPX 300 spectrometer operating at 300.13 MHz and at room temperature. ^{13}C NMR spectra were recorded at 75.47 MHz. Samples were prepared by dissolving ca. 10 mg of (1*R*,3*S*,4*S*,8*S*)-*p*-menthane-3,9-diol (Scheme 2) in 0.5 mL of deuteriochloroform containing 0.03% (v/v) of TMS as an internal reference. GC−MS spectra were obtained on a HP GC/MS System 5988A by EI ionizaion at 70 eV. IR spectra were recorded on a Perkin-Elmer 1600FT.

Scheme 2. Synthesis of (1*R*,3*S*,4*S*,8*S*)-*p*-Menthane-3,9-diol

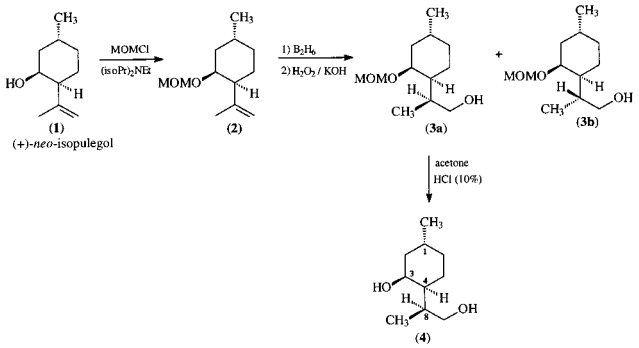

(1*R*,3*S*,4*S*)-3-Methoxymethyl-*p*-menthane (2). To a solution of (+)-*neo*-isopulegol (**1**) (0.4871 g; 3.15 mmol) in dry CH_2Cl_2 (15 mL) and chloromethyl methyl ether (0.29 mL; 3.79 mmol), mantained at 0 °C under nitrogen atmosphere was added dropwise *N*,*N*-diisopropylethylamine (1.1 mL; 6.3 mmol). The resultant mixture was stirred at room temperature for 4 h. The reaction mixture was diluted with ethyl acetate, and the organic phase was washed twice with saturated aqueous sodium bicarbonate solution and twice with saturated aqueous sodium chloride solution. The organic phase was separated, dried with $MgSO_4$, and concentrated under vacuum. The crude product was purified by column chromatography on silica gel eluting with hexane/ethyl acetate (9:1) to yield compound **2** (0.5321 g; 86%) as a colorless liquid. ^{1}H NMR ($CDCl_3$), δ (ppm): 0.82 (d, J = 6.5 Hz, 3H), 1.02 (m, 3H), 1.76 (m, 3H), 1.79 (s, 3H), 1.92 (m, 1H), 3.26 (s, 3H), 3.92 (broad s, 1H), 4.51 (d, J = 6.4 Hz, 1H), 4.64 (d, J = 6.4 Hz, 1H), 4.74 (m, 1H), 4.81 (m, 1H). ^{13}C NMR ($CDCl_3$), δ (ppm): 22.3 (CH_3); 22.4 (CH_3); 24.9 (CH_2); 26.4 (CH); 34.9 (CH_2); 39.5 (CH_2); 47.9 (CH); 55.2 (CH_3); 73.8 (CH); 95.3 (CH_2) 110.5 (CH_2); 147.3 (C). MS *m*/*z* (rel intensity): 138 (4), 121 (8), 94 (13), 45 (100), 42 (10). IR (film) (cm^{-1}): 1042, 1147, 1643, 3080.

(1*R*,3*S*,4*S*,8*S*)-3-Methoxymethyl-*p*-menthan-9-ol (3a). Diborane generated from $NaBH_4$ (0.1092 g; 2.87 mmol) and $BF_3{\cdot}Et_2O$ (0.35 mL; 2.87 mmol) in diglyme was passed through a solution of compound **2** (0.1903; 0.96 mmol) in dry THF (6 mL) maintained at 0 °C. After addition of diborane, the reaction mixture was stirred for 4 h at room temperature. Then, THF (1 mL of a 50% aqueous solution) was added to the reaction mixture. The resultant solution was cooled at 0 °C, and then KOH (1 mL of a 12% ethanolic solution) and H_2O_2 (0.5 mL of a 30% aqueous solution) were added and the resulting mixture was stirred for 0.5 h. The product was extracted with ethyl acetate, and the organic phase was washed with water, dried with $MgSO_4$, and concentrated under vacuum. The crude product was purified by column chromatography on silica gel eluting with hexane/ethyl acetate (7:3) to yield two epimers: compound **3a** (0.1350 g; 65%) and compound **3b** (0.0451 g; 21.7%) as colorless liquids. Compound **3a**. ^{1}H NMR ($CDCl_3$), δ (ppm): 0.86 (d, J = 6.5 Hz, 3H), 0.93 (m, 3H), 1.03 (d, J = 7.2 Hz, 3H), 1.27 (m, 1H), 1.43 (m, 1H), 1.62 (m, 1H), 1.68 (m, 1H), 1.73 (m, 1H), 2.01 (m, 1H), 2.90 (broad s, 1H), 3.28 (s, 3H), 3.46 (dd, J = 11.8 Hz and J = 0.6 Hz, 1H), 3.83 (dd, J = 11.8 Hz and J = 1.9 Hz, 1H), 3.95 (broad s, 1H), 4.66 (d, J = 4.5 Hz, 1H), 4.79 (d, J = 4.5 Hz, 1H). ^{13}C NMR ($CDCl_3$), δ (ppm): 16.6 (CH_3); 22.3 (CH_3); 22.9 (CH_2); 26.3 (CH); 35.0 (CH_2); 37.5 (CH); 38.6 (CH_2); 44.8 (CH); 56.0 (CH_3); 65.6 (CH_2); 75.0 (CH); 95.0 (CH_2). MS *m*/*z* (rel intensity): 167 (49), 153 (86), 137 (36), 109 (23), 95 (55), 45 (100). IR (film) (cm^{-1}): 1039, 1151, 3415.

(10) Malkin, V. G.; Malkina, O. L.; Steinebrunner; Huber, H. *Chem. Eur. J.* **1996**, *2*, 452.
(11) Dev, S. In *Terpenoids Handbook*; CRC Press: Boca Raton, FL, 1985.
(12) Namba, A. M.; León, S.; da Silva, G. V. J.; Alemán, C. *Tetrahedron* **2000**, *56*, 6089.

Compound **3b.** ^{1}H NMR ($CDCl_3$), δ (ppm): 0.86 (d, $J = 6.6$ Hz, 3H), 0.87 (m, 3H), 0.98 (d, $J = 7$ Hz, 3H), 1.26 (m, 1H), 1.51 (m, 2H), 1.73 (m, 2H), 1.98 (m, 1H), 2.90 (broad s, 1H), 3.48 (s, 3H), 3.52 (d, $J = 4.9$ Hz, 2H), 3.93 (broad s, 1H), 4.59 (d, $J = 4.5$ Hz, 1H), 4.73 (d, $J = 4.5$ Hz, 1H). ^{13}C NMR ($CDCl_3$), δ (ppm): 15.2 (CH_3); 22.3 (CH_3); 24.7 (CH_2); 26.3 (CH); 35.2 (CH_2); 37.3 (CH); 38.7 (CH_2); 43.5 (CH); 55.9 (CH_3); 65.7 (CH_2); 73.9 (CH); 95.2 (CH_2). MS *m*/*z* (rel intensity): 199 (29), 153 (48), 95 (45), 71 (15), 45 (100). IR (film) (cm^{-1}): 1093, 1147, 1039, 3409.

(1*R*,3*S*,4*S*,8*S*)-*p*-Menthane-3,9-diol (4). To a solution of compound **3a** (0.1350 g; 0.62 mmol) in acetone (4 mL) was added HCl (1 mL of a 10% aqueous solution). The resultant solution was stirred at room temperature for 4 h. The acetone was removed under vacuum, and the crude product was dissolved in CH_2Cl_2 (15 mL) and washed twice with saturated aqueous sodium bicarbonate solution, twice with saturated aqueous sodium chloride solution, and with water. The organic phase was separated, dried with $MgSO_4$, and concentrated under vacuum. The crude product was purified by column chromatography on silica gel eluting with hexane/ethyl acetate (6:4) to yield compound **4** (0.0943 g; 87.7%) as a colorless liquid.

On the basis of ^{1}H, ^{13}C, and COSY NMR spectra, the hydrogen and carbon atoms of **4** were assigned. The ^{13}C chemical shifts of this compound were validated through HBMC and HMQC NMR experiments. The data are summarized in Tables 1 and 2 of the Supporting Information.

Force-Field Calculations. MD simulations in chloroform solution were carried out using the program package AMBER 4.0.[13,14] The force-field parameters used in this work were taken from a previous study.[15] The (1*R*,3*S*,4*S*,8*S*)-*p*-menthane-3,9-diol molecule was placed in the center of an equilibrated box of chloroform molecules with density 1.48 g/mL. The solvent molecules that overlapped the (1*R*,3*S*,4*S*,8*S*)-*p*-menthane-3,9-diol were discarded. The resulting system had dimensions of 25.60 × 25.60 × 25.60 Å^3 and contained 125 chloroform molecules. The OPLS model was used to describe the chloroform molecules.[16] Periodic boundary conditions were applied using the nearest image convention. We updated the list of nonbonding interactions every 25 steps, and imposed an 8 Å cutoff for these interactions. Accordingly, the simulation boxes are large enough to mimic a dilute solution. The SHAKE algorithm[17] was used to constrain bond lengths of the solvent molecules to their equilibrium values.

After initial minimization of the whole system, MD simulation was begun with initial velocities set to zero. The system was coupled to a thermal bath using the algorithm developed by Berendsen et al.,[18] which applied a velocity scaling at each step. The system was heated to 300 K in 25 ps using a temperature coupling parameter of 0.2 ps in a constant volume simulation. The time step was 0.001 ps, and the coordinates were stored every 1000 steps. The simulation was run for a total of 3 ns after 25 ps of equilibration.

Quantum Mechanical Calculations. The most relevant conformations provided by MD simulations have been used to predict NMR properties of the (1*R*,3*S*,4*S*,8*S*)-*p*-menthane-3,9-diol molecule. The electronic structure of these conformations was determined using density functional theory (DFT) methods, which include some electron correlation effects not present at the Hartree−Fock level. More specifically, the Becke[19] three-parameter hybrid functional with gradient corrections provided by the LYP functional[20] (B3LYP) was used. The Kohn−Sham orbitals were constructed using Gaussian-type atomic orbital (AO) basis sets. All the calculations were performed using the 6-311G(d) basis set[21] to describe the C, H, and O atoms of the molecule under study.

Carbon isotropic shielding constants of (1*R*,3*S*,4*S*,8*S*)-*p*-menthane-3,9-diol, $\sigma(^{13}C_i)_{diol}$, were computed using perturbation theory and the Gauge Invariant Atomic Orbitals (GIAO) method[4] implemented in the Gaussian 94 program package.[22] Chemical shifts, $\delta(^{13}C_i)$, are referred to a usual standard as TMS through the relation

$$\delta(^{13}C_i) = \sigma(^{13}C)_{TMS} - \sigma(^{13}C_i)_{diol} \quad (1)$$

where, to have accurate chemical shifts, the isotropic shielding constant of carbon atoms in TMS, $\sigma(^{13}C)_{TMS} = 184.2$ ppm, was computed at the same level of calculation described above.[23]

Solvent effects in NMR parameters were taken through the supermolecule approach by including explicit solvent molecules in the study. Thus, calculations of the wave functions and of nuclear shieldings were carried out on (1*R*,3*S*,4*S*,8*S*)-*p*-menthane-3,9-diol−*n*$CHCl_3$ complexes, where *n* ranges from 3 to 16. The position of the chloroform molecules around the solute was chosen by analyzing the solvent configurations obtained in MD simulations. Small basis sets were used for the atoms of the chloroform molecules by the following two reasons: (i) the size of the (1*R*,3*S*,4*S*,8*S*)-*p*-menthane-3,9-diol and (ii) the large number of explicit solvent molecules involved in this study. Specifically, the chloroform molecules included in the complexes were described using the STO-3G,[24] 3-21G,[25] and 3-21G(d)[26] basis sets.

The statistical evaluation of the similarity between experimental and calculated chemical shifts was carried out considering (i) the scaling coefficient (*c*) and the Pearson correlation coefficient (*r*) for a fitting of the type $y = cx$ and (ii) the root-mean-square deviation (rms).

Both force-field and quantum mechanical calculations were performed at the Centre de Supercomputació de Catalunya (CESCA).

Results

Molecular Dynamics Simulations. Molecular Conformation. Two chair conformations can be predicted for the compound under study (Scheme 3). The first one presents the methyl and 1-methyl-2-hydroxyethyl substituents in equatorial position and the hydroxyl substituent in axial position (**I**). Calculations using different theoretical methods clearly indicated that this conformation is several kcal/mol more stable than the other one with the methyl and 1-methyl-2-hydroxyethyl substituents in axial positions (**II**). Therefore, conformer **I** was used as starting point for MD simulations.

(13) Weiner, S. J.; Kollman, P. A.; Nguyen, D. T.; Case, D. A. *J. Comput. Chem.* **1986**, *7*, 230.
(14) Pearlman, D. A.; Case, D. A.; Caldwell, J. W.; Ross, W. S.; Cheatham, T. E., III; Ferguson, D. M.; Seibel, G. L.; Singh, U. C.; Weiner, P. K.; Kollman, P. A. Amber 4.1, University of California, San Francisco, 1995.
(15) Namba, A. M.; León, S.; da Silva, G. V. J.; Alemán, C. *J. Comput. Aided. Mol. Design*. **2000**, in press.
(16) Jorgensen, W. L.; Briggs, J. M.; Contreras, M. L. *J. Phys. Chem.* **1990**, *94*, 1683.
(17) Ryckaert, J.-P.; Ciccotti, G.; Berendsen, H. J. C. *J. Comput. Phys.* **1977**, *23*, 327.
(18) Berendsen, H. J. C.; Postma, J. P. M.; van Gunsteren, W. F.; DiNola, A.; Haak, J. R. *J. Chem. Phys.* **1984**, *81*, 3684.
(19) Becke, A. D. *J. Chem. Phys.* **1993**, *98*, 5648.
(20) Lee, C.; Yang, W.; Parr, R. G. *Phys. Rev. B* **1988**, *37*, 785.
(21) McLean, A. D.; Chandler, G. S. *J. Chem. Phys.* **1980**, *72*, 5639.
(22) Gaussian 94, Revision B.3., Frisch, M. J.; Trucks, H. B.; Schlegel, H. B.; Gill, P. M. W.; Johnson, B. G.; Robb, M. A.; Cheeseman, J. R.; Keith, T.; Petersson, G. A.; Montgomery, J. H. B.; Schlegel, H. B.; Gill, P. M. W.; Johnson, B. G.; Robb, M. A.; Cheeseman, J. R.; Keith, T.; Petersson, G. A.; Montgomery, J. A.; Raghavachari, K.; Al-Laham, M. A.; Zakrzewski, V. G.; Ortiz, V. G.; Foresman, J. B.; Peng, C. Y.; Ayala, P. Y.; Chen, W.; Wong, M. W.; Andres, J. L.; Replogle,.G.; Foresman, J. B.; Peng, C. Y.; Ayala, P. Y.; Chen, W.; Wong, M.W.; Andres, J. L.; Replogle, le, E. S.; Gomperts, R.; Martin, R. L.; Fox, D. J.; Binkley, J. S.; Defrees, D. J.; Baker, J.; Stewart, J. J. P.; Head-Gordon, M.; Gonzalez, C.; Pople, J. A. Gaussian, Inc., Pittsburgh, PA, 1995.
(23) Casanovas, J.; Pacchioni, G.; Illas, F. *Mater. Sci. Eng. B* **1999**, *68*, 16.
(24) Hehre, W. J.; Stewart, R. F.; Pople, J. A. *J. Chem. Phys.* **1969**, *51*, 2657.
(25) Binkley, J. S.; Pople, J. A.; Hehre, W. J. *J. Am. Chem. Soc.* **1980**, *102*, 939.
(26) Krishnan, R.; Pople, J. A. *Int. J. Quantum Chem.* **1978**, *14*, 91.

Scheme 3. Chair Conformations of (1*R*,3*S*,4*S*,8*S*)-*p*-Menthane-3,9-diol

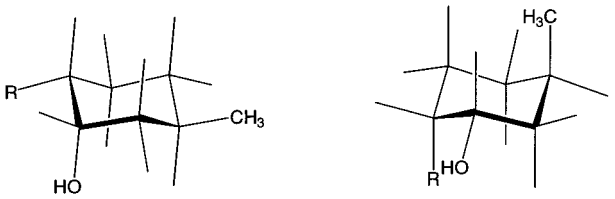

R= 1-methyl-2-hydroxy-ethyl

I **II**

Figure 1a represents the variation with time of the torsional angles C1−C2−C3−O, C2−C3−C4−C8, and C5−C6−C1−C7 obtained during the MD simulation. The most immediately noticeable feature is the large stability of the chair conformation used as starting point. Thus, it remains essentially unaltered along the entire trajectory and no transition toward another conformation is detected. On the other hand, the evolution of the dihedral angles C3−C4−C8−C9 and C4−C8−C9−O, which is displayed in Figure 1b, have been used to describe the conformational preferences of the 1-methyl-2-hydroxyethyl substituent. The *gauche*$^+$ is the most populated conformation for the dihedral angle C3−C4−C8−C9, although it changes to *gauche*$^-$ after 900 ps. However the latter conformation transforms again into the former one in about 1200 ps. It is worth noting that the *gauche*$^+$ and *gauche*$^-$ conformations avoid unfavorable steric interactions between the ring and the 1-methyl-2-hydroxyethyl substituent.

On the other hand, the conformational preferences of the dihedral angle C4−C8−C9−O are led by the formation of a hydrogen bonding interaction between the two hydroxyl groups. As can be seen in Figure 1b, C4−C8−C9−O changes with C3−C4−C8−C9 allowing to preserve such intramolecular interaction. Thus, the former changes from *gauche*$^-$ to *gauche*$^+$ when the conformation of the latter varies from *gauche*$^+$ to *gauche*$^-$. Figure 1c shows the preferences for the two hydroxyl groups, the predominant conformations for the dihedral angles C2−C3−O−H and C8−C9−O−H being the trans and *skew*$^-$, respectively. It is interesting to note the C8−C9−O−H dihedral angles changes from *skew*$^-$ to *gauche*$^+$ around 800 ps and retains the latter conformation by about 1300 ps. This conformational transition is related with a swap in the hydrogen bonding pattern, in which the two hydroxyl groups interchange their donor and acceptor roles.

A list with the population of the unique conformations of (1*R*,3*S*,4*S*,8*S*)-*p*-menthane-3,9-diol was organized. Conformations were discarded by comparing the dihedral angles of both the cyclohexane ring and the substituents with the corresponding dihedrals of the conformations already listed. A conformation was kept if at least one of the dihedral angles differed in more than 30°; otherwise, the conformation was rejected. Results indicated that two conformations (Figure 2), denoted **A** and **B**, are the most populated ones, i.e., about 31% and 23%, respectively,

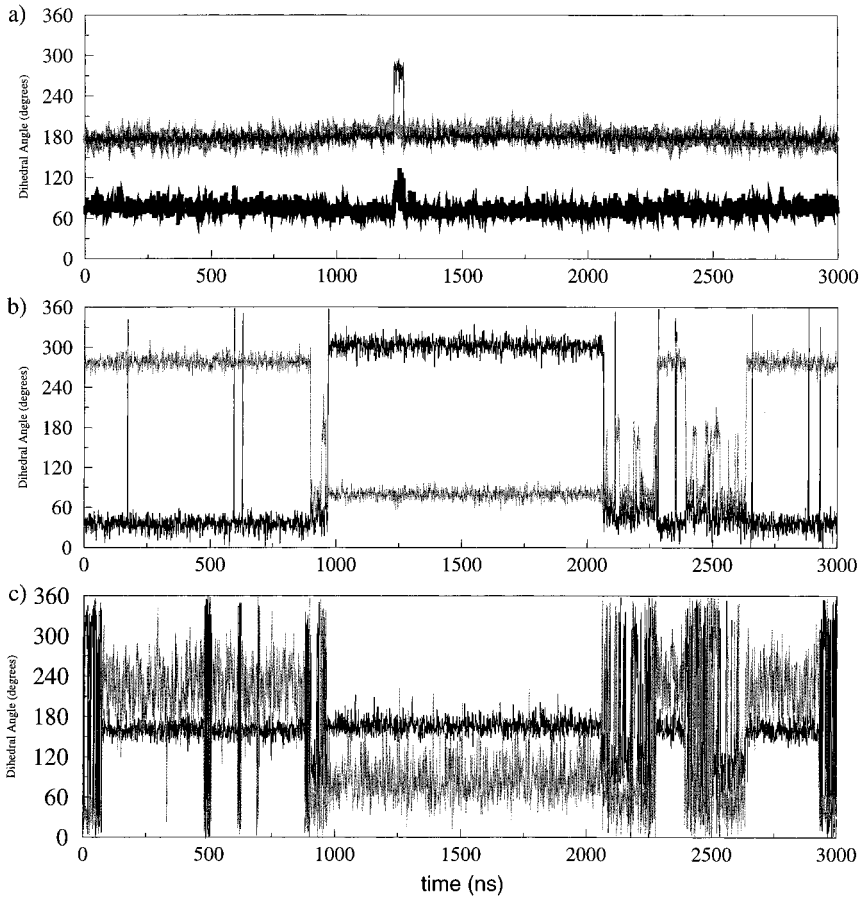

Figure 1. Trajectory plots of the torsional angles: (a) C1−C2−C3−O (thick dark line), C2−C3−C4−C8 (thick gray line) and C5−C6−C1−C7 (thin dark line); (b) C3−C4−C8−C9 (dark line) and C4−C8−C9−O (gray line); and (c) C2−C3−O−H (dark line) and C8−C9−O−H (gray line); as observed for (1*R*,3*S*,4*S*,8*S*)-*p*-menthan3-3,9-diol from MD simulations in chloroform solution.

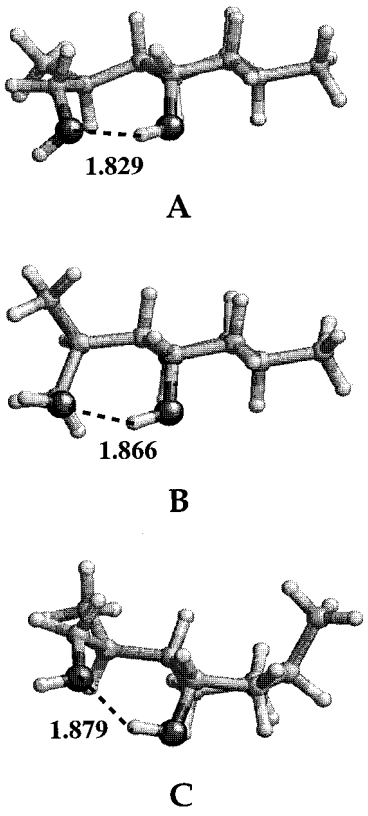

Figure 2. View of the conformations selected for NMR chemical shifts calculations. These conformations were the most populated in MD simulations (see text). Distances (in Å) between the hydrogen bonded hydroxyl groups are indicated.

the population of the remaining 19 unique conformations being lower than 7%. Accordingly, conformations **A** and **B** were selected for NMR chemical shifts calculations. As can be seen in Figure 2, these two conformations are stabilized by an intramolecular hydrogen bond which is in good agreement with previous experimental results.[12] Thus, ^{1}H NMR spectra of (1*R*,3*S*,4*S*,8*S*)-*p*-menthane-3,9-diol in deuterated chloroform exhibited an intramolecular interaction involving the hydroxyl groups. The dihedral angles of the two conformations are listed in the Supporting Information. As expected from the results displayed in Figure 1, they mainly differ in the arrangement of the 1-methyl-2-hydroxyethyl substituent.

On the other hand, conformation **II** (see Scheme 3) was used as starting geometry of a 500 ps MD simulation. This initial arrangement becomes into a twist conformation in 50 ps, which transforms into the chair conformation I after 300 ps. The unique conformations of the resulting trajectory were selected using the procedure described in the previous paragraph. The most populated twist conformation (more than 40%), which was denoted **C**, presents the 1-methyl-2-hydroxyethyl and hydroxyl substituents in equatorial and axial positions, respectively. This conformation is also displayed in Figure 2 and was used to explore the differences in NMR chemical shifts between the most stable chair and twist conformations of the cyclohexane ring.

Distribution of the Solvent around the Solute. Figure 3 presents the computed radial pair distribution function, *rpdf(r)*, of chloroform atoms about the atoms of (1*R*,3*S*,4*S*,8*S*)-*p*-menthane-3,9-diol. No sharp peak associated to a well-defined first hydration shell was found.

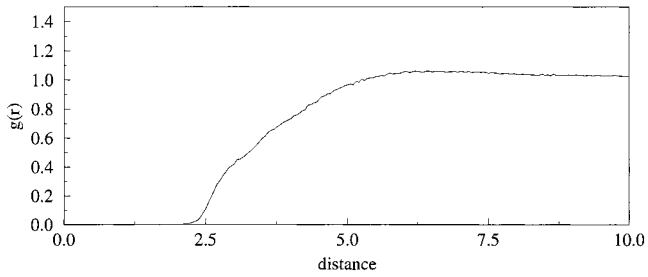

Figure 3. Radial pair distribution function, *rpdf(r)*, of chloroform atoms about the atoms of (1*R*,3*S*,4*S*,8*S*)-*p*-menthane-3,9-diol.

Table 1. Theoretical Chemical Shifts (δ; in ppm) of ^{13}C for the Most Populated Conformations of (1*R*,3*S*,4*S*,8*S*)-*p*-Menthane-3,9-diol[a]

	conformation A				conformation B			
	isolated		complex		isolated		complex	
atom no.	δ	$\Delta\delta$	δ	$\Delta\delta$	δ	$\Delta\delta$	δ	$\Delta\delta$
C1	29.4	3.2	28.3	2.1	25.0	−1.2	26.4	0.2
C2	44.7	2.4	43.8	1.5	42.0	−0.3	41.1	−1.2
C3	69.1	2.6	67.8	1.3	70.1	3.6	69.9	3.4
C4	44.4	−1.6	42.4	−3.6	46.8	0.8	46.9	0.9
C5	28.8	3.4	26.6	1.2	28.2	2.8	28.1	2.7
C6	36.0	0.6	37.2	1.8	36.4	1.0	38.4	3.0
C7	24.3	1.9	24.6	2.2	21.2	−1.1	21.0	−1.4
C8	42.3	4.2	38.2	0.1	38.6	0.5	35.5	−2.6
C9	68.8	3.8	62.7	−2.3	63.8	−1.2	62.1	−2.8
C10	15.3	−0.6	17.5	1.6	16.3	0.4	17.4	1.5

[a] The values listed correspond to those obtained for the isolated molecule and the complex with all the solvent molecules at a distance closer than 4.5 Å (see text; the structures of these complexes are displayed in Figure 5). The solvent molecules are described with the STO-3G basis set. Differences with respect to the experimental values (Table 3) ($\Delta\delta$; in ppm) are also displayed.

Moreover, analysis of the maximum residence time for the chloroform molecules nearest to the solute reveal that they have a large mobility and exchange very rapidly with the bulk chloroform. According to this, the chloroform molecules required for chemical shift calculations were chosen using a distance criterion, the *rpdf(r)* being used to find the solvent molecules closest to the solute.

NMR Chemical Shifts of the Isolated Molecule. Prior to study in depth, the environment effects, NMR chemical shifts of carbon atoms in (1*R*,3*S*,4*S*,8*S*)-*p*-menthane-3,9-diol, $\delta(^{13}C_i)$, were computed considering the isolated molecule in the gas-phase. The carbon chemical shifts evaluated for conformations **A** and **B** at the B3LYP/6-311G(d) level of calculation are displayed in Table 1. The statistical data in Table 2 demonstrate excellent agreement between experimental and theoretical values. Thus, Pearson correlation coefficients are $r = 0.99$ with rms values of about 2−3 ppm. It should be noted that for conformation **A** the similarity between experimental and theoretical data is excellent for all the carbon atoms with exception of C1, C5, C8, and C9, which are overestimated by about 3−4 ppm. The chemical shifts measured for these four carbon atoms are better reproduced by **B** than by **A**. Moreover, for conformation **B** the only value overestimated by more than 3 ppm is the chemical shift of C3. Indeed, our statistical analysis indicates that **B** provides better results, in general, than **A**.

On the other hand, carbon chemical shits calculated for conformation **C** (data not shown) indicated that the change from chair to twist implies a considerable deterioration in the agreement between the theoretical and

Table 2. Statistical Results[a] of the Comparison between the Experimental and Theoretical NMR Chemical Shifts in (1*R*,3*S*,4*S*,8*S*)-*p*-Menthane-3,9-diol

environment	conf A	conf B	conf C
isolated diol at the B3LYP/6-311G(d) level	0.99	0.99	0.97
	1.05	**1.02**	**0.97**
	2.7	*1.7*	*4.3*
diol at the B3LYP/6-311G(d) level + 3 $CHCl_3$ around the polar region at the STO−3G level	1.00	0.99	
	1.02	**1.01**	
	1.8	*1.7*	
diol at the B3LYP/6-311G(d) level + 3 $CHCl_3$ around the nonpolar region at the STO−3G level	0.99	0.99	
	1.06	**1.02**	
	3.4	*1.8*	
diol at the B3LYP/6-311G(d) level + 3 $CHCl_3$ around the polar region at the 3−21G level	1.00	0.99	
	1.03	**1.01**	
	2.0	*1.7*	
diol at the B3LYP/6-311G(d) level + 3 $CHCl_3$ around the polar region at the 3-21G(d) level	1.00	0.99	
	1.03	**1.01**	
	2.0	*1.7*	
diol at the B3LYP/6-311G(d) level + 6 $CHCl_3$ at the STO-3G level	0.99	0.99	
	1.03	**1.02**	
	2.6	*2.6*	
diol at the B3LYP/6-311G(d) level + all the $CHCl_3$ molecules at a distance closer than 4.5 Å described at the STO−3G level	0.99	0.99	
	1.00	**1.01**	
	1.9	*2.2*	

[a] Standard font indicates the Pearson correlation coefficient, bold font indicates the scaling coefficient, and italic font indicates the root-mean-square deviation (rms; in ppm).

experimental chemical shifts (Table 2). Accordingly, conformation **C** was not considered in the analysis of the solvent effects.

NMR Chemical Shifts in Chloroform Solution. Solvent-induced changes in $\delta(^{13}C_i)$ were estimated using the supermolecule approach. More specifically, we investigated the influence of (i) the position of the solvent molecules around the solute, (ii) the basis set used to describe the solvent, and (iii) the number of explicit solvent molecules.

Dependence on the Position of the Solvent Molecules around the Solute. As was mentioned in the Introduction, *p*-menthane-3,9-diols are amphiphilic molecules with the polar and nonpolar regions clearly defined. The influence of the chloroform molecules arranged in each region on the chemical shifts was investigated by considering complexes constituted by (1*R*,3*S*,4*S*,8*S*)-*p*-menthane-3,9-diol and three solvent molecules. The position of the solvent molecules around these regions was taken from the MD trajectories previously shown. Thus, the chloroform molecules closest to the solute were used for these calculations. Figure 4 shows the arrangement of the solvent molecules around the polar and nonpolar regions for the conformations **A** and **B** of (1*R*,3*S*,4*S*,8*S*)-*p*-menthane-3,9-diol. The calculated NMR chemical shifts for these four complexes are listed in Table 3, the statistical analyses of the results being included in Table 2. Calculations were performed considering the 6-311G(d) and STO-3G basis sets for the (1*R*,3*S*,4*S*,8*S*)-*p*-menthane-3,9-diol and chloroform molecules, respectively.

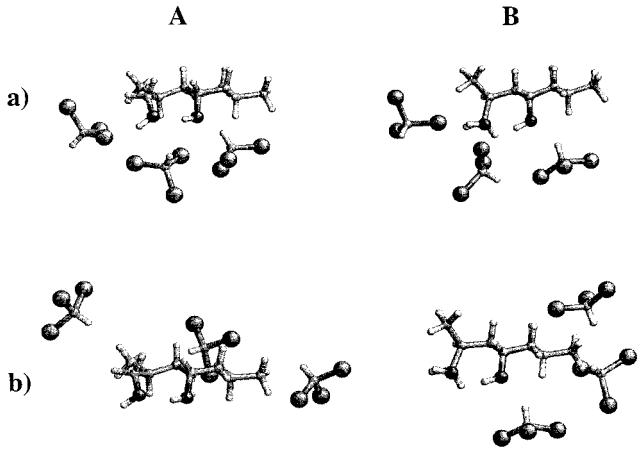

Figure 4. View of the complexes selected for NMR chemical shifts calculations on conformations **A** and **B** of solvated (1*R*,3*S*,4*S*,8*S*)-*p*-menthane-3,9-diol. Complexes contain three solvent molecules around the polar (a) or nonpolar (b) regions of the solute.

As can be seen, the agreement between the experimental chemical shifts and those predicted for conformation **A** improves when the solvent molecules are distributed around the polar region. Thus, the rms is lower than that obtained for the isolated molecule by 0.9 ppm. Furthermore, there is also an improvement in the scaling and Pearson correlation coefficients. However, when the chloroform molecules are located at the nonpolar region of **A**, the statistical parameters are similar, or even worst, than those obtained for the isolated molecule. A different situation appears for conformation **B** since the chemical shifts predicted for the isolated molecule are very similar to those obtained for the complex with three solvent molecules, independently of their position around the solute. Thus, no clear improvement is induced by explicitly considering the three solvent molecules around this conformation.

Effect of the Basis Set on the Description of the Solvent. The importance of the basis set used to describe the solvent in the supermolecule approximation was investigated by considering the complexes containing three chloroform molecules around the polar region of the solute (Figure 4a). For this purpose, calculations were performed using the STO-3G, 3-21G, and 3-21G(d) basis sets for the solvent, whereas the solute was described in all cases with the 6-311G(d) basis set. The statistical analysis of the results has been included in Table 2, and the $\delta(^{13}C_i)$ predicted with the 3-21G(d) basis set are listed in Table 3.

Comparison of the results displayed in Tables 2 and 3 indicates that the effect of the basis set is similar for conformation **A** and **B**. Thus, the chemical shifts predicted for the two conformations with the three basis sets are very similar suggesting that the STO-3G basis set is able to capture the solvent effects. Furthermore, it is worth noting that the two conformations present a similar agreement with experimental when solvent effects are included.

Effect of the Number of Explicit Solvent Molecules. To ascertain the influence of the number of explicit solvent molecules on $\delta(^{13}C_i)$ calculations, we investigated complexes with more than three solvent molecules. First, complexes with six chloroform molecules were generated by joining those closest to the polar and nonpolar regions

Table 3. Theoretical Chemical Shifts (in ppm) of ^{13}C for the Complexes Constituted by (1*R*,3*S*,4S,8*S*)-*p*-Menthane-3,9-diol and Three Solvent Molecules[a] Distributed around Either the Polar or Nonpolar Regions of the Solute

	conformation A			conformation B			
	polar		nonpolar	polar		nonpolar	
atom	STO-3G	3-21G(d)	STO-3G	STO-3G	3-21G(d)	STO-3G	exptl
C1	28.9	29.1	29.4	26.1	26.4	26.1	26.2
C2	44.9	45.1	44.5	41.8	41.7	41.6	42.3
C3	69.6	69.8	69.1	70.2	70.2	70.2	66.5
C4	44.6	44.9	44.4	46.7	46.7	46.6	46.0
C5	26.6	27.7	29.3	28.5	28.4	28.1	25.4
C6	35.9	35.8	40.8	36.1	36.1	38.0	35.4
C7	23.9	23.9	26.5	21.1	21.2	20.8	22.4
C8	38.3	39.6	42.1	38.5	38.5	38.5	38.1
C9	64.7	65.5	68.7	63.2	63.5	63.7	65.0
C10	14.2	14.4	16.2	16.3	16.2	16.3	15.9

[a] The solvent molecules are described using the STO-3G and 3-21G(d) basis sets, as indicated in the columns. Experimental values (in ppm) are listed in the last column for comparison. The complexes are displayed in Figure 4.

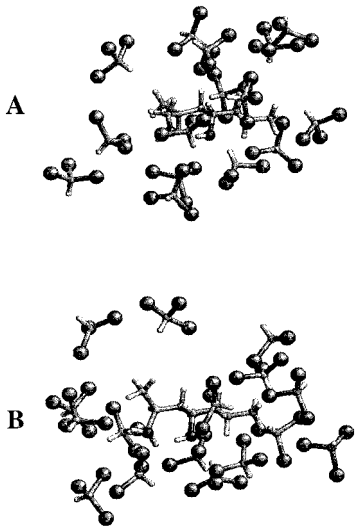

Figure 5. Conformations **A** and **B** of (1*R*,3*S*,4*S*,8*S*)-*p*-menthane-3,9-diol surrounded by 15 and 16 chloroform molecules.

of the solute; i.e., for each conformation the solvent molecules displayed in Figure 4a,b were joined. The chemical shifts (data not shown) obtained for these complexes did not provide any improvement with respect to those obtained with less solvent molecules. Indeed, the statistical analysis of the results, which has been included in Table 2, indicates that the new NMR parameters are similar or even worst than those calculated for the complexes with only three solvent molecules.

As a final step, we decided to evaluate the NMR chemical shifts of (1*R*,3*S*,4*S*,8*S*)-*p*-menthane-3,9-diol but considering a number of solvent molecules enough to mimic the solution state. This was done by selecting all the chloroform molecules arranged at less than 4.5 Å of the solute, i.e., a complete solvation shell. The resulting systems are displayed in Figure 5. It is worth noting that now 15 and 16 explicit chloroform molecules surround conformations **A** and **B**, respectively. The computed chemical shifts and the results of the statistical analysis are listed in Tables 1 and 2, respectively.

It should be mentioned that calculations took more than 100 h each on an IBM-SP2 computer. Results reveal a small improvement of the chemical shifts predicted for conformation **A**. Thus, scaling coefficients indicate that the error associated to the predicted chemical shifts is lower than that obtained for the molecule in the gas phase and with three solvent molecules around the polar region by 5% and 2%, respectively. On the other hand, no improvement was obtained for conformation **B**. Accordingly, it can be concluded that the large computational cost of calculations with a complete solvation shell is not compensated by a significant improvement of the chemical shifts.

Discussion

The ^{13}C NMR chemical shifts of (1*R*,3*S*,4*S*,8*S*)-*p*-menthane-3,9-diol have been calculated using a combination of MD simulations and quantum chemical calculations, the resulting values being compared with experimental data. MD simulations were used to investigate the conformational preferences of (1*R*,3*S*,4*S*,8*S*)-*p*-menthane-3,9-diol in chloroform solution. Results allowed to identify the most populated conformations of this molecule, which correspond to two chair conformations with the methyl and 1-methyl-2-hydroxyethyl substituents in equatorial position and the hydroxyl substituent in axial position. Chemical shifts were computed for such conformations as well as for a less populated twist conformation at the B3LYP/6-311G(d) level using the GIAO method.

The computed chemical shifts depend strongly on the conformation, the agreement with experimental data being better for the chair conformations than for the twist one. The rms for the former conformations is lower than 3 ppm whereas for the latter is larger than 4 ppm. Indeed, for conformation **A** the agreement between the theoretical and experimental chemical shifts is very good for all the carbon atoms excepting C1, C5, C8 and C9. For conformation **B** only the chemical shift predicted for C3 differs by more than 3 ppm with respect to the experimental value. The discrepancies found for these atoms are largely improved by including solvent effects. Thus, when conformation **A** is surrounded by chloroform molecules only C4 presents a difference between the calculated and the experimental values larger than 3 ppm.

The effects of the solvent on the chemical shifts have been analyzed using the supermolecule approach. Thus, complexes constituted by the (1*R*,3*S*,4*S*,8*S*)-*p*-menthane-3,9-diol and a different number of chloroform molecules have been generated for each conformation. The position of the solvent molecules around the solute was taken from the MD results. The analysis of the calculated

chemical shifts for the smallest complexes, in which three chloroform molecules are considered, revealed an improvement of the results. This improvement is more notorious for conformation **A** than for conformation **B**. Thus, when the surrounding solvent molecules are distributed around the polar region of conformation **A**, the best agreement between experimental and theoretical chemical shifts is reached.

The small differences found for the solvated conformations may be due to several sources of error. The first one is the level of theory at which the geometry of (1*R*,3*S*,4*S*,8*S*)-*p*-menthane-3,9-diol was determined. Thus, computed chemical shifts are considerably influenced by the geometric parameters, i.e., bond lengths and angles.[1d] In this case, the molecular geometry was taken from a force-field explicitly designed to study *p*-menthane-3,9-diols.[15] Other sources of error in the calculation of $\delta(^{13}C_i)$ may be the level of theory used and, at a lesser extend, the quality of the basis set used to describe the (1*R*,3*S*,4*S*,8*S*)-*p*-menthane-3,9-diol molecule. Electron correlation effects largely influence the NMR parameters[1d,9,27] These effects are partially included in B3LYP calculations at a reasonable computational cost. Indeed, DFT methods allow calculations on large organic systems, like (1*R*,3*S*,4*S*,8*S*)-*p*-menthane-3,9-diol, that cannot be treated by conventional correlated methods. However, it should keep in mind that better results can be obtained with other correlated methods such as MP2.[28] On the other hand, the choice of the basis set is a crucial decision in any quantum mechanical calculation. For reliable calculations of chemical shifts, there is a need for flexibility in the outer-core inner-valence regions.[1d,29] However, such basis sets lead to more time-consuming calculations and in practice cannot be applied to large organic molecules.

It should be also mentioned that the experimentally measured $\delta(^{13}C_i)$ refer to a hypothetical average conformation of (1*R*,3*S*,4*S*,8*S*)-*p*-menthane-3,9-diol. MD simulations indicate that this is a quite flexible compound, the number of unique conformations being 21. Our calculations were performed considering the most populated conformations, i.e., **A** and **B**, which represent a population of about 54%. The remaining conformations were neglected since they appeared during very short periods. However, these 19 conformations present a total population of 46%, even although the population of each conformation is lower than 7%. Thus, the consideration of the low populated conformations could improve the predicted chemical shifts. Moreover, it should be considered that the molecule spends some time moving between these conformations, this effect being recorded by NMR experiments but not by the calculations.

Conclusions

^{13}C NMR chemical shifts, $\delta(^{13}C_i)$, of (1*R*,3*S*,4*S*,8*S*)-*p*-menthane-3,9-diol were experimentally measured and computed using a combination of MD simulations and quantum mechanical calculations. MD simulations were used to explore the conformational preferences of this molecule in chloroform solution. The NMR parameters were calculated in the gas phase and in chloroform solution. The solvent effects were considered using the supermolecule approach, where the arrangement of the chloroform molecules around the solute was provided by MD simulations. Calculations were performed with the B3LYP method, which partially collects the effects of correlation, the basis sets used to describe the (1*R*,3*S*,4*S*,8*S*)-*p*-menthane-3,9-diol and the solvent molecules being the 6-311G(d) and STO-3G, respectively. Following this theoretical strategy, we found that the chemical shifts calculated for the most populated conformations compare favorably with the experimental values. The agreement between theoretical and experimental $\delta(^{13}C_i)$ improves when chloroform molecules are distributed around the polar region of (1*R*,3*S*,4*S*,8*S*)-*p*-menthane-3,9-diol. The computational strategy used in this work seems to be a promising tool for both predicting and interpreting NMR spectra of complex organic molecules.

Acknowledgment. We thank the CESCA (Centre de Supercomputació de Catalunya) for computational facilities. We also wish to thank the Fundação de Amparo à Pesquisa do Estado de São Paulo (FAPESP) and Coordenadoria de Aperfeiçoamento de Pessoal de Nível Superior (CAPES) for financial support.

Supporting Information Available: Tables of ^{1}H and ^{13}C NMR shifts, dihedral angles, and complete computational results. This material is available free of charge via the Internet at http://pubs.acs.org.

JO0016982

(27) Stanton, J. F.; Gauss, J.; Siehl, H. U. *Chem. Phys. Lett.* **1996**, *262*, 183.
(28) Cheeseman, J. R.; Trucks, G. W.; Keith, T. A.; Frisch, M. J. *J. Chem. Phys.* **1996**, *104*, 5497.
(29) Carmichael, I. *J. Phys. Chem.* **1993**, *97*, 1789.